Published in final edited form as:

Nature. 2014 November 6; 515(7525): 138–142. doi:10.1038/nature13601.

Broad and potent HIV-1 neutralization by a human antibody that binds the gp41-120 interface

Jinghe Huang[1], **Byong H. Kang**[1], **Marie Pancera**[2], **Jeong Hyun Lee**[3,4], **Tommy Tong**[5], **Yu Feng**[4], **Ivelin S. Georgiev**[2], **Gwo-Yu Chuang**[2], **Aliaksandr Druz**[2], **Nicole A. Doria-Rose**[2], **Leo Laub**[1], **Kwinten Sliepen**[6], **Marit J. van Gils**[6], **Alba Torrents de la Peña**[6], **Ronald Derking**[6], **Per-Johan Klasse**[7], **Stephen A. Migueles**[1], **Robert T. Bailer**[2], **Munir Alam**[8], **Pavel Pugach**[7], **Barton F. Haynes**[8], **Richard T. Wyatt**[4], **Rogier W. Sanders**[6,7], **James M. Binley**[5], **Andrew B. Ward**[3,4], **John R. Mascola**[2], **Peter D. Kwong**[2], and **Mark Connors**[1]

[1]HIV-Specific Immunity Section, Laboratory of Immunoregulation, National Institute of Allergy and Infectious Diseases, National Institutes of Health, Bethesda, Maryland 20892, USA [2]Vaccine Research Center, National Institute of Allergy and Infectious Diseases, National Institutes of Health, Bethesda, Maryland 20892, USA [3]Department of Integrative Structural and Computational Biology, The Scripps Research Institute, La Jolla, California, USA [4]The Scripps Center for HIV/AIDS Vaccine Immunology and Immunogen Discovery, The Scripps Research Institute, La Jolla, California 92037, USA [5]San Diego Biomedical Research Institute, San Diego, California, USA [6]Department of Medical Microbiology, Academic Medical Center, University of Amsterdam, Amsterdam, The Netherlands [7]Department of Microbiology and Immunology, Weill Medical College of Cornell University, New York, New York 10065, USA [8]Duke Human Vaccine Institute, Duke University, Durham, North Carolina 27710, USA

Correspondence and requests for materials should be addressed to M.C. (mconnors@nih.gov).

Supplementary Information is available in the online version of the paper.

Author Contributions M.C., J.H., B.K., M.P., J.R.M., P.D.K., J.B., R.T.W., R.W.S., J.P.M., and A.B.W. each contributed to the design of the study, analysis of the data, and preparation of this manuscript. J.H. and B.K. performed B-cell sorting, antibody cloning, neutralization assays, cell surface staining, and epitope mapping assays. M.P., J.H.L., A.B.W., and P.D.K. performed the structural studies. L.L. cultured B cells and assisted with recovery of IgG genes. N.R. performed the 35O22 biotinylation and provided data of PG9, PG16, PGT121 and PGT128 breadth and potency. P.-J.K. performed SPR experiments. R.D., K.S., A.T.d.l.P., and P.P. performed the ELISA BG505 SOSIP.664 mutants. M.J.v.G. performed neutralization assays with HIV_{LAI} viruses. S.M.A. and B.F.H. performed the autoreactivity assays. I.S.G. and G.Y.C. performed serologic analysis. M.P. and P.D.K. performed 35O22 crystallographic analysis. J.H.L. and A.W. performed the negative stain EM studies. J.B. and T.T. planned and performed the antibody competition, and HIV VLP entry studies. Y.F. and R.W. planned and performed the washout and kinetic studies. S.A.M. led the clinical care of the patients. R.T.B. screened the B-cell culture supernatants for neutralization activity.

The 35O22 heavy and light chain plasmids and antibody have been submitted to the NIH-AIDS reagent program. The nucleotide sequence of 35O22 and its variants have been submitted to GenBank under accession numbers KM001872-KM001879 (heavy chain) and KM001880-KM001887 (light chain). Coordinates and structure factors for 35O22 Fab has been deposited with the Protein Data Bank under accession code 4TOY. The reconstruction of BG505 SOSIP.664 in complex with 35O22 Fab has been deposited in the Electron Microscopy Data Base under accession code EMD-2672.

The authors declare no competing financial interests. Readers are welcome to comment on the online version of the paper.

Abstract

The isolation of human monoclonal antibodies (mAbs) is providing important insights regarding the specificities that underlie broad neutralization of HIV-1 (reviewed in[1]). Here we report a broad and extremely potent HIV-specific mAb, termed 35O22, which binds novel HIV-1 envelope glycoprotein (Env) epitope. 35O22 neutralized 62% of 181 pseudoviruses with an IC_{50}<50 μg/ml. The median IC_{50} of neutralized viruses was 0.033 μg/ml, among the most potent thus far described. 35O22 did not bind monomeric forms of Env tested, but did bind the trimeric BG505 SOSIP.664. Mutagenesis and a reconstruction by negative-stain electron microscopy of the Fab in complex with trimer revealed it to bind a conserved epitope, which stretched across gp120 and gp41. The specificity of 35O22 represents a novel site of vulnerability on HIV Env, which serum analysis indicates to be commonly elicited by natural infection. Binding to this new site of vulnerability may thus be an important complement to current mAb-based approaches to immunotherapies, prophylaxis, and vaccine design.

Induction of a potent neutralizing antibody response capable of recognizing highly diverse isolates of HIV-1 is among the very most important goals of HIV vaccine research. This represents a considerable challenge given the extraordinary antigenic variability of the Env surface glycoprotein. However, approximately 20% of the HIV-infected population does develop a humoral immune response capable of recognizing highly diverse strains[2–6]. In the past several years improved patient cohorts[2–6], HIV-specific B cell isolation[7–9], and IgG cloning techniques [10,11] have permitted extraordinary progress in isolation of broadly neutralizing monoclonal antibodies (bNabs) from these individuals. Thus far, these primarily fall into four categories based upon the position of their epitopes on the Env protein, a trimer of gp120 and gp41 heterodimers that is the target of neutralizing antibodies. These sites include the CD4-binding site on gp120[8,12] (of which VRC01 is an example), the glycan-containing regions of V1V2 on gp120 (of which PG9 and PG16 are examples), the V3 region centered on the N332 glycan of gp120[7,13] (of which PGT121 is an example) and the membrane-proximal external region (MPER) on gp41 (of which 10E8 is an example)[14,15]. It remains unclear to what extent these four categories represent the prevalent and immunodominant sites of Env vulnerability through which broad neutralizing responses are mediated, or whether additional specificities exist[16–19]

Here we report the isolation of a broad and potently neutralizing HIV-specific mAb, 35O22, that binds a novel epitope. The neutralizing activity of 35O22 is highly complementary to the activities of other known bNabs. We used mutagenesis, crystallography and EM to define the Env site targeted by 35O22. Our results indicate that 35O22 neutralization occurs by a novel mode of trimer recognition along a conserved face on contiguous areas of gp41 and gp120.

To further understand the specificities that underlie broadly neutralizing antibody responses we applied a technique to identify human mAbs of interest from peripheral blood B cells without prior knowledge of the target specificity[9]. IgG^+ B cells of a donor (N152), with broad and potent neutralizing serum and from whom recently described 10E8 antibody was cloned[20], were sorted and expanded. The supernatants of B cell microcultures were screened for neutralizing activity and IgG genes from positive wells were cloned and re-expressed. In

addition to the 10E8 antibody, 8 clonal family variants of an additional antibody with neutralization activity were found, among which the 35O22 antibody was the most potent and broad (Supplementary Table 1a,b). This antibody was derived from *IGHV-1-18*02*- and *IGLV-2-14*02* germline genes, and was highly somatically mutated in variable genes of both heavy chain (35%) and λ light chain (24%) compared to germline. The 35O22 antibody possessed a heavy-chain complementarity-determining 3 region (CDR H3) composed of 14 amino acids (Fig. 1a and Supplementary Table 2) and an insertion of 8 amino acids in framework 3 (FR3). High levels of somatic mutation and FR3 insertions are features of other HIV-specific bNabs[7–9,12,13,21,22]. Autoreactivity or polyreactivity are properties of several HIV-specific antibodies[23,24] that could limit their use in therapies or prophylaxis. However, 35O22 bound Hep-2 epithelial cells only modestly (Extended Data Fig. 1a) and did not bind a panel of autoantigens (Extended Data Fig. 1b,c). Against a large panel of pseudoviruses, 35O22 neutralized 62% of 181 isolates with an IC_{50}<50 μg/ml (Fig. 1b and Supplementary Table 3). In numerous cases where the IC_{50} of 10E8 was >1 μg/ml, that of 35O22 was 100 to 1000-fold lower (Supplementary Table 1b and Supplementary Table 3), indicating their activities were highly complementary. It is likely that 35O22-like antibodies account for much of the breadth and potency of the N152 patient serum against clades A and B (Supplementary Table 3), whereas 10E8-like antibodies may account for much of the breadth against clade C isolates. Overall, the median IC_{50} of 35O22 for sensitive viruses was 0.033 μg/ml, which is among the most potent thus far described (Fig. 1b).

The neutralizing spectrum of 35O22 was then compared to those of other bNabs. The IC_{50} of 35O22 against a panel of diverse isolates did not correlate with those of the bNabs VRC01, 10E8, PG9, and PGT121 (Extended Data Fig. 2a). In addition, a neutralization-based clustering analysis revealed that 35O22 clustered separately from other bNabs (Extended Data Fig. 2b). Further, 35O22 did not compete with other known bNabs when bound to virus-like particles (VLPs) (Extended Data Fig. 2c). Its neutralization of many pseudoviruses did not exceed 80% even at high concentrations (Extended Data Fig. 3a) and its potency increased when pseudoviruses were produced in the presence of the glycosidase inhibitors NB-DNJ or kifunensine, consistent with recognition of high mannose (Extended Data Fig. 3b)[25]. However, neutralization was unaffected by mutation of *N*-linked glycosylation sites critical for binding of known bNabs (Extended Data Fig. 4c) [7,13]. Taken together these data suggested that 35O22 binds glycans, but its specificity differed from all previously characterized bNabs.

Mutation of four predicted sites of *N*-linked glycosylation on HIV_{JRCSF} Env diminished neutralization potency; N88A, N230A, N241A, and N625A (Fig. 2a and Supplementary Table 4). This result suggested that 35O22 recognized elements of both gp120 and gp41, a property that may be consistent with several very recently isolated antibodies [16–19]. When mutations were introduced in the 5 residues on either side of these four sites, the V89A, T90A, K227A, T232A, and S243A mutations each diminished neutralization (Supplementary Table 4). With the exception of V89A and K227A, it is likely the impact of each of these mutations was to disrupt the Asn-X-Ser/Thr glycotransferase sequon. There was no impact of T627A suggesting a glycan may not be present at 625 and 35022 may make a protein contact at this position. Overall, similar results were obtained using

replication competent HIV_{LAI} viruses (Supplementary Table 5). Examination of the sequences of resistant pseudoviruses within clade C did not reveal a clear pattern of variation at each of the positions found to affect 35O22 neutralization or within the glycosylation sequon. It is therefore possible that the resistance of clade C viruses is mediated by other factors such as variations in glycosylation pattern or conformation.

35O22 did not bind to a panel of soluble recombinant Env proteins (Extended Data Fig. 5a, b, c) suggesting these do not have the appropriate conformation or glycosylation for binding. However, the 35O22 antibody did bind a recently described stabilized, cleaved, soluble trimer, BG505 SOSIP.664 (Fig. 2b)[26], Despite a plateau in neutralization below 50% (Extended Data Fig. 3a) and lacking glycans at positions 230 and 241, binding to BG505 SOSIP.664 trimer had numerous characteristics consistent with its activity against the HIV_{JRCSF} pseudovirus. 35O22 binding was increased to trimer produced in cells treated with kifunensine or cells deficient in glycan processing, and diminished by mutations at positions 88 and 625 (Fig. 2c). 35O22 did bind to BG505 SOSIP trimer lacking the furin cleavage site (BG505 SOSIP.SEKS). In surface plasmon resonance (SPR) experiments, 35O22 also bound to immobilized BG505 SOSIP.664 with high affinity (K_d=5.6nM) (Fig. 2d). Binding was markedly lower to the gp120-41_{ECTO} protomer and no binding was detected to the gp120 monomer (Fig. 2e). It bound the uncleaved BG505 SOSIP.SEKS but no binding was observed to the uncleaved form lacking the SOSIP mutations (Fig. 2f). These observations, combined with the lack of binding of 35O22 to all other soluble forms of Env tested, suggested this antibody requires a trimeric structure for binding its epitope on gp120 and gp41[27].

To provide an atomic-level understanding of the structure of the 35O22 antibody, we crystallized the Fab of 35O22. Crystals were obtained that diffracted to 1.55Å resolution (Supplementary Table 6). Overall the structure of 35O22 Fab revealed a relatively flat antigen-combining site, lacking long protruding loops, and flanked by the complementarity-determining region 1 on the light chain (CDRL1) and the 8 amino acid insertion in FR3 of the heavy chain (Fig. 3a). The surface of the antigen combining site was heavily altered by somatic mutation and two pairs of cysteines introduced by somatic mutation in CDR L1 and L3 formed disulphide bonds (Fig. 3a and Extended Data Fig. 6a).

We next sought to determine the structure of the antibody-antigen complex. The ability of 35O22 to bind the BG505 SOSIP.664 trimer permitted imaging of the antibody-antigen complex by negative stain electron microscopy (EM). The reconstruction of these images showed that three 35O22 Fabs bound to the trimers at sites close to the predicted viral membrane (Fig. 3b and Extended Data Fig. 6b). Superposition of the negative stain reconstruction of the soluble BG505 SOSIP.664 with 35O22 Fab onto the BaL EM tomogram of the viral spike (Extended Data Fig. 6b) suggested the viral membrane to be in close contact to the 35O22 Fab light chain. Tyr68 and Trp69 in the light chain and FR3 tyrosines at residues 65 and 72 form potential surfaces of membrane association. The 35O22 heavy chain was in close proximity to the four sites observed to contribute to the 35O22 epitope in mutagenesis experiments (N88, N234, N241 and N625). The CDR H3 was predicted to interact with N625 and CDRH2 with N88. The 8 amino acid insertion in the framework 3 heavy chain is located close to residues 88–90 on gp120. Reversion of this

insertion to germline markedly diminished neutralization against most pseudoviruses in our panel (Supplementary Table 7). 35O22 binds a surface on the Env spike that is distinct from two other antibodies, 8ANC195 and PGT151, reported to bind gp120 and gp41 (Extended Data Fig. 7) [16–18].

Analysis of the 35O22 site of vulnerability (Extended Data Fig. 8a–c) indicated it was highly conserved. The glycans predicted at positions 88, 241, and 625 were found to be among the most highly conserved *N*-linked glycosylation sequons of 4265 HIV-1 sequences in the Los Alamos database (Supplementary Table 8). Despite this high level of conservation, analysis of the Env gene of the patient's plasma virus showed that the predicted amino acid sequence varied at the critical 35O22 contacts. In addition to the previously published 10E8 escape mutations, an N230Q is predicted in one sequence, N241D in half of the sequences, and an N624D and N625Q in all sequences (Extended Data Fig. 9a). When these mutations were introduced into HIV_{JRCSF} pseudoviruses there was a drop in neutralization with the greatest effect caused by the N625Q mutation found in all of the plasma sequences (Extended Data Fig. 9b). These data suggest that the autologous virus has escaped neutralization by 35O22.

To gain insight into the prevalence of the 35O22 specificity, we added the 35O22 neutralization fingerprint to the 10 that we had previously identified (Extended Data Fig. 8d–e)[28]. Notably, 13 of the sera (38%) showed significant 35O22-neutralization signals (>0.2). This level of prevalence was substantially higher than for the V1V2-directed response (typified by the PG9 antibody) or that of the 8ANC195 antibody. However, it was lower than the prevalence of responses to the MPER (50% prevalence), the CD4-binding site (56% prevalence), or the V3 glycan site (82% prevalence). The neutralizing activity of sera was also measured against HIV_{JRCSF} pseudoviruses bearing N88A, N230A, N241A, or N625A mutations (Extended Data Table 1). These mutations caused a greater than 5-fold increase in ID_{50} in more than half of donors, with a high level of concordance between the impact of each of these mutations within a given serum. These results suggested that 35O22 is unlikely to be the product of a unique B cell repertoire or infecting virus, but rather arises commonly among patients that develop HIV-specific neutralizing antibodies.

To better understand the mechanism of 35022's activity, we examined the timing of its binding and neutralization during virus fusion. Given the proximity of the 35O22 epitope to the membrane, it was important to perform these experiments in the context of Env expressed on cells or virions. In these settings, MPER-specific antibodies have limited access to the native trimer and bind best after the conformational changes induced by CD4 attachment[29]. Binding of 35O22 to Env expressed on the cell surface was low and similar to the MPER antibody 2F5 (Fig. 4a). 35O22 binding to VLPs was weak compared to that of VRC01 but similar to that of 10E8 (Fig. 4b). 35O22 binding was slightly inhibited by sCD4 binding, suggesting the 35O22 epitope is not induced by sCD4 under these experimental conditions. 35O22 neutralization was partially eliminated by washing of pseudovirions prior to infection, a result consistent with limited access to Env on free virions (Fig. 4c)[29]. However, if 35O22 was incubated with VLPs, permitted to bind to target cells, and then after 2 hours the cells were washed, there was little impact on neutralization similar to all other antibodies except the MPER 10E8 antibody (Fig. 4d). Similar to 2G12 and 10E8,

35O22 activity was relatively high in the post-CD4 format, consistent with prior work showing that virus-sCD4 complexes are more sensitive to neutralization than virus alone[30]. In a post-CD4/CCR5 assay, only 10E8 neutralized, consistent with prior observations (Fig. 4d) [30]. Taken together with the structural data, these results suggest that in the context of a lipid membrane, 35O22 binds Env poorly prior to CD4 attachment. However, following trimer attachment to CD4, 35O22 binds to an early intermediate that exposes the 35O22 epitope possibly by raising the Env spike within the viral membrane (Fig. 4e).

The 35O22 antibody and its specificity have a number of implications for the use of antibodies in HIV therapy, prophylaxis, and efforts to stimulate HIV-specific antibodies with vaccines. Its novel binding site and spectrum of activity against HIV strains suggest it could complement other antibodies used in passive immunotherapy or prophylaxis. In addition, the antibody is extremely potent suggesting its activity *in vivo* may therefore persist even at low concentrations. Perhaps most importantly, the novel epitope bound by the 35O22 antibody represents a new site of vulnerability that could potentially be targeted by HIV vaccines. The high prevalence of 35O22-like neutralizing activity in HIV-infected cohorts, increases the likelihood that production of similar antibodies could be induced by vaccination. In addition, the highly specific recognition by 35O22 of BG505 SOSIP.664 suggests that this soluble, cleaved trimer antigenically resembles the native Env trimer at the gp120-gp41 interface. Given the binding characteristics of 35O22, these results underscore the possibility that immunogens structurally similar to the native trimer are required for elicitation of such antibodies[27].

METHODS

Study patients

We selected the plasma and peripheral blood mononuclear cells (PBMCs) from the HIV-1-infected patients enrolled in the National Institute of Health under a clinical protocol (ClinicalTrials.gov identifier NCT00029445) approved by the Investigational Review Board in the National Institute of Allergy and Infectious Diseases (NIAID-IRB). All participants signed informed consent approved by the NIAID-IRB. The criteria for enrolment were as follows: having a detectable viral load, a stable CD4 T-cell count above 400 cells μl^{-1}, being diagnosed with HIV infection for at least 4 years, and off antiretroviral treatment for at least 5 years. Donor N152 was selected for B-cell sorting and antibody generation because his serum neutralizing activity is among the most potent and broad in our cohort. At the time of leukapheresis, he had been infected with HIV-1 for 20 years, with CD4 T-cell counts of 325 cells μl^{-1}, plasma HIV-1 RNA values of 3,811 copies ml^{-1} and was not on antiretroviral treatment.

Memory B-cell staining, sorting and antibody cloning

Staining and single-cell sorting of memory B cells were performed following a detailed protocol recently published[9]. Briefly, a total of 140,000 $CD19^{+}IgA^{-}IgD^{-}IgM^{-}$ memory B cells were sorted and re-suspended in medium with IL-2, IL-21 and irradiated 3T3-msCD40L feeder cells, and seeded into 384-well microtitre plates at a density of 4 cells per well. After 13 days of incubation, supernatants from each well were screened for

neutralization activity using a high-throughput micro-neutralization assay against HIV-$1_{MN.3}$ and HIV-$1_{Bal.26}$. From the wells that scored positive in both the HIV-$1_{MN.3}$ and HIV-$1_{Bal.26}$ neutralization assay the variable region of the heavy chain and the light chain of the immunoglobulin gene were amplified by RT–PCR and re-expressed as described previously[10]. The full-length IgG was purified using a recombinant protein-A column (GE Healthcare).

Generation of pseudoviruses and VLPs

HIV-1 Env pseudoviruses were generated by co-transfection of 293T cells with pSG3 delta Env backbone and a second plasmid that expressed HIV-1 Env at a ratio of 2:1. 72 h after transfection, supernatants containing pseudoviruses were harvested and frozen at −80 °C until further use. Glycosidase-inhibitors were added to the cells at the time of transfection at flowing concentration, 25 μM kifunensine, 500 μM NB-DNJ and 20 μM swainsonine. JRCSF mutants were produced by altering the JRCSF Env plasmid using QuikChange Lightning mutagenesis according to the manufacturer's protocol (Agilent). VLPs for ELISA assays were produced by transient transfection of 293T cells with a pCAGGS Env-expressing plasmid and the subgenomic plasmid pNL4-3.Luc.R-E- as previously described[31].

Neutralization assays

Neutralization activity of monoclonal antibodies or serum was measured using single-round HIV-1 Env-pseudovirus infection of TZM-bl cells as described previously[32]. HIV-1 Env pseudoviruses were generated by co-transfection of 293T cells with an Env-deficient backbone (pSG3ΔEnv) and an expression plasmid for the Env gene of interest. HIV_{LAI} viruses were generated by transfection of a single plasmid containing the entire viral genome. At 72 h after transfection, supernatants containing pseudovirus were harvested and frozen at −80 °C until further use. In the neutralization assay, heat-inactivated patient serum or monoclonal antibody was serially diluted five fold with Dulbecco's modified Eagle medium–10% FCS (Gibco), and 10 μl was incubated with 40 μl of pseudovirus in a 96-well plate at 37 °C for 30 min. TZM-bl cells were then added and plates were incubated for 48h. Assays were then developed with a luciferase assay system (Promega), and the relative light units (RLU) were read on a luminometer (Perkin Elmer). Washing of pseudovirions to determine access by antibody to the trimer on free virus was performed as described previously[33]. Neutralization in various formats to determine the timing and mechanism of neutralization were performed as described previously[30,34]. Briefly, in the standard "leave in" format monoclonal antibodies were mixed with VLPs 1h prior to infection of CF2.CD4.CCR5 cells with no subsequent washing. Alternatively, in a "cell wash" format, virus and antibody were incubated with target cells for 2h, followed by a wash to remove any unattached virus. In the post-CD4 format, VLPs were premixed with 3 μg/ml of sCD4 for 15 min., then incubated with antibody for 1h before adding to cells that lack CD4 but express CCR5 (CF2.syn.CCR5 cells). In the post-CD4/CCR5 format, SOS VLPs were permitted to attach to cells for 2h, unbound VLPs were washed away and graded concentrations of antibodies were added before infection was activated with DTT.

Prediction of prevalence of 35O22-like antibodies in patient serum

An antibody neutralization fingerprint, the pattern with which an antibody neutralizes a panel of diverse viral strains, was used to delineate the structural epitope recognized by that antibody [28,35]. For each serum, neutralization on a panel of 21 HIV-1 strains was represented as a combination of the neutralization fingerprints for a reference set of antibody specificities targeting the other four major sites of Env vulnerability as well as the 35O22 fingerprint, to obtain an estimate of the relative contribution of each of these specificities to neutralization by the given serum. The neutralization behavior of sera was deconvoluted from a cohort of 34 donors, each with neutralization breadths of greater than 50%.

Binding assays

HIV_{YU2} gp160 extracellular domain (gp140) foldon trimer, gp120 and gp41 monomers were produced as described previously[36]. HIV_{BaL}(clade B), HIV_{CM235} (CRF01_AE), HIV_{CN54} (clade C), $HIV_{96ZM651}$ (clade C), $HIV_{93TH975}$ (clade E) gp120 proteins; and the HIV_{UG37} (clade A), HIV_{CN54} (clade C), HIV_{UG21} (clade D) and HIV_{BR29} (clade F) gp140 monomers were obtained through the NIH AIDS Research and Reagent Program. For ELISA assays each antigen (2 μg ml^{-1})was coated on 96-well plates overnight at 4 °C. Plates were blocked with BLOTTO buffer (PBS, 1% FBS, 5% non-fat milk) for 1 h at room temperature, followed by incubation with antibody serially diluted in disruption buffer (PBS, 5% FBS, 2% BSA, 1% Tween-20) for 1 h at room temperature. 1:10,000 dilution of horseradish peroxidase (HRP)-conjugated goat anti-human IgG antibody was added for 1 h at room temperature. Plates were washed between each step with 0.2% Tween 20 in PBS. Plates were developed using 3,3′,5,5′-tetramethylbenzidine (TMB) (Sigma) and read at 450 nm. ELISA assays using the BG505 SOSIP.664 trimer and mutants were performed as described previously[26,27]. Surface plasmon resonance experiments were performed at 25°C on a Biacore 3000 instrument (GE Healthcare) using D7324 or anti-Histidine capture as previously described[37]. For the SPR experiment presented in Fig. 2d an anti-histidine capture was used (R_L= ~500 RU) and in Fig. 2e,f a D7324 capture was used (R_L = ~150 RU for trimer and protomer; 130 RU for gp120 in 2e and R_L = ~500 RU in 2f). ELISA assays using VLPs were performed as previously described[30,31].

Autoreactivity assays

Reactivity to HIV-1 negative human epithelial (HEp-2) cells was determined by indirect immunofluorescence on slides using Evans Blue as a counterstain and FITC-conjugated goat anti-human IgG (Zeus Scientific)[23]. Slides were photographed on a Nikon Optiphot fluorescence microscope. Kodachrome slides were taken of each monoclonal antibody binding to HEp-2 cells at a 10-s exposure, and the slides scanned into digital format. The Luminex AtheNA Multi-Lyte ANA test (Wampole Laboratories) was used to test for monoclonal antibody reactivity to SSA/Ro, SS-B/La, Sm, ribonucleoprotein (RNP), Jo-1, double-stranded DNA, centromere B, and histone and was performed as per the manufacturer's specifications and as previously described[23]. Monoclonal antibody concentrations assayed were 50, 25, 12.5 and 6.25 μg ml^{-1}. 10 μl of each concentration were incubated with the luminex fluorescent beads and the test performed per the manufacturer's specifications.

Structure determination and analysis

The antigen-binding fragment of 35O22 (Fab) was prepared using HRV3C digestion, as previously described[38]. HRV3C was introduced in the hinge region of the heavy chain plasmid DNA. Both light and heavy chain plasmids were cotransfected in 293F as described previously. The antibody, 35O22 with HRV3C IgG was purified over protein A, cleaved with HRV3C and the flow-through collected and run onto a size-exclusion chromatography (S200). Purified 35O22 Fab set up for 20 °C vapour diffusion sitting-drop crystallizations on the Honeybee 963 robot. A total of 576 initial conditions adapted from the commercially available Hampton (Hampton Research), Precipitant Synergy (Emerald Biosystems) and Wizard (Emerald Biosystems) crystallization screens were set up and imaged using the Rockimager (Formulatrix), followed by hand optimization of crystal hits. Crystals were grown in 15% isopropanol, 25% PEG 3350, 0.2 M Ammonium citrate pH 4.5 diffracted to 1.55 Å resolution in a cryoprotectant composed of mother liquor supplemented with15% 2*R*-3*R*-butanediol. After mounting the crystals on a loop, they were flash cooled and data were collected at 1.00 Å wavelength at SER CAT ID-22 beamlines (APS) and processed using HKL-2000 [39]. Structures were solved through molecular replacement with Phaser [40,41], using a previously obtained free structure of VRC01 germline as a search model. Structure solution identified one Fab per asymmetric unit in a $P4_12_12$ lattice. Refinement of the structure was undertaken with Phenix, with iterative model building using Coot[42]. Refinement resulted in an R_{cryst} value of 16.65% (R_{free}=18.22%). The structure was validated with MolProbity[43], yielding 98.1% and 100 % of residues falling within most favoured Ramachandran regions and allowed Ramachandran regions, respectively. All graphics were prepared with Pymol (PyMOL Molecular Graphics System).

Electron microscopy and image processing

Negative stain EM grids were prepared as previously stated [44]. Data were collected using a FEI Tecnai T12 electron microscope operating at 120 keV, with an electron dose of ~30 e^{-}/Å^2 and a magnification of 52,000× that resulted in a pixel size of 2.05 Å at the specimen plane. Images were acquired with a Tietz TemCam-F416 CMOS camera using a nominal defocus range of 800 to 1000 nm using the Leginon interface (ref). Image processing was carried out as described previously [45]. The final reconstruction was performed using 4746 unbinned particles, refining for 40 iterations with C3 symmetry applied. The resulting density was ~19 Å resolution at a Fourier shell correlation (FSC) cut-off of 0.5. Fab fitting was carried out using the Fit function in Chimera, using 0.0115 contour level for the map. The Fab orientation where the heavy chain is towards gp120 (as shown in Figure 3b) was chosen on the basis of the two correlation coefficients (0.95)(471 of 7058 atoms outside contour). vs. 0.91 (1012 of 7058 atoms outside contour). In the alternate orientation (light chain towards gp120), the FR3 insertion did not fit within the density. The man-9 glycans were modeled onto the BG505 SOSIP.R6.664 (PDB ID 4NCO)[46] using the GLYCAM-Web server(http://www.glycam.com). Dominant sites of vulnerability to neutralizing antibody elicited during chronic infection in Extended Data Fig. 8 is shown in the context of an EM tomogram from the BAL viral spike [47].

Extended Data

a

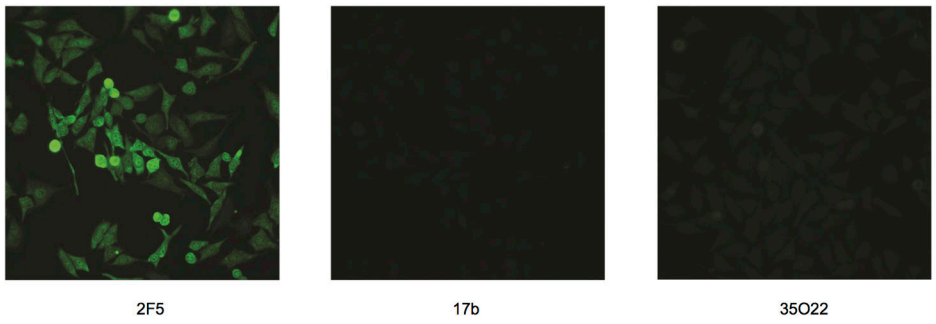

b

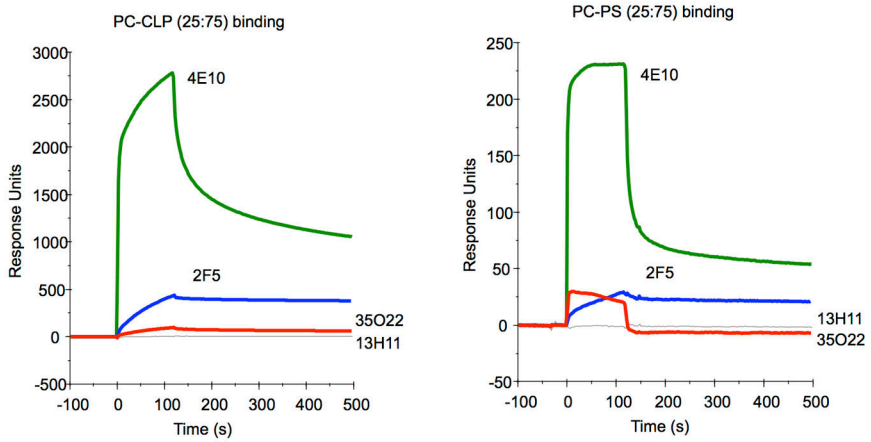

c

Sample ID	SSA	SSB	Sm	RNP	Scl 70	Jo 1	dsDNA	Cent B	Histone
Neg Control	-	-	-	-	-	-	-	-	-
Pos Control 1								273	
Pos Control 2	521	856				336	1036		409
Pos Control 3			658	340	322				
synagis	3	6	5	5	3	1	9	2	3
4E10	90	206	24	12	7	196	14	11	46
35O22	8	8	7	6	3	47	0	2	7

Extended Data Figure 1. Analysis of 35O22 autoreactivity

a, Reactivity of 35O22 with HEP-2 epithelial cells. 2F5 was used as a positive control and 17b as a negative control. Antibody concentration was 25 μg/ml. All pictures are shown at 400x magnification. **b**, SPR analysis of 35O22 binding to anionic phospholipids. 35O22 was injected over PC-CLP liposomes or PC-PS liposomes immobilized on the BIAcore L1 sensor chip. 4E10 and 2F5 were used as positive controls and 13H1 as a negative control. **c**, Reactivity of 35O22 with autoantigens detected in Luminex assay. 4E10 was used as a positive control. Synagis, an anti-RSV monoclonal antibody, was used as a negative control. SSA, Sjogren's syndrome antigen A; SSB, Sjogren syndrome antigen B; Sm, Smith antigen; RNP, ribonucleoprotein; Scl 70, scleroderma 70; Jo1, antigen; CentrB, centromere B. A positive response is >120 units.

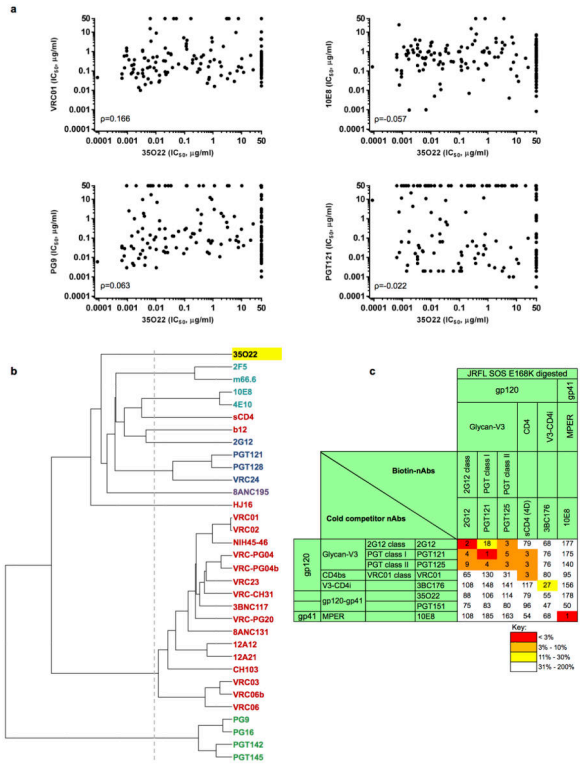

Extended Data Figure 2. Neutralization similarities between 35O22 and other HIV-1 bNAbs

a, Correlation (Spearman) between the neutralization potencies of 35O22 and the indicated antibody against 172 pseudoviruses. Representatives from all four major sites of vulnerability are shown. Resistant strains corresponding to values of >50 µg/ml are plotted as 50. **b**, Neutralization-based clustering of bNabs over a set of 172 diverse HIV-1 strains. A putative epitope-specific clustering cutoff is shown as a dashed line. Antibodies are colored according to the respective target site of vulnerability: red (CD4bs), blue (glycan-V3), V1V2 (green), light blue (MPER), and other (purple). 35O22 (yellow) clusters separately from all other antibodies, indicating a novel mechanism of neutralization. **c**, 35O22 competition with other bNAbs on HIV_{JRFL} VLPs with the trimer stabilizing SOS mutations in an ELISA assay. Biotin-bNAbs were titrated into the ELISA at increasing concentrations in the presence of excess (10 µg ml^{-1}) cold competitor neutralizing antibodies. Values in the table indicates percentage binding of biotin-nAbs in the presence of cold-competitor. ND = not done

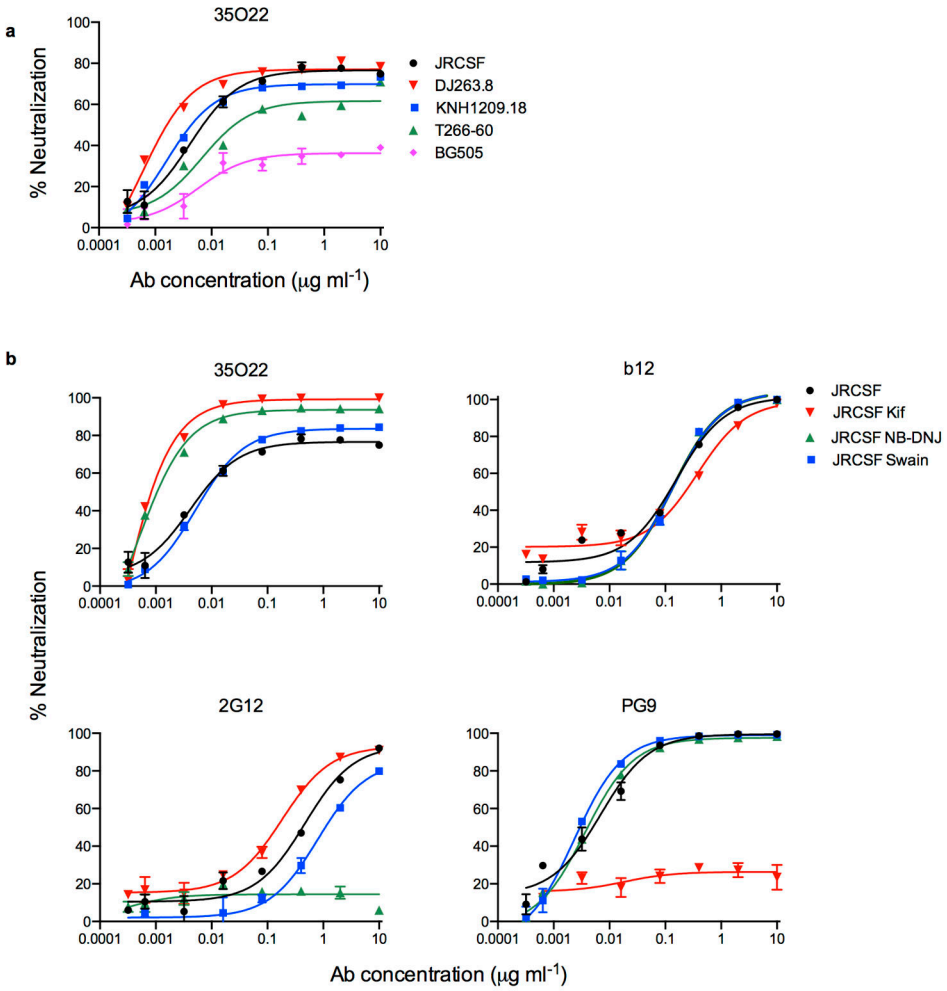

Extended Data Figure 3. 35O22 binds to N-linked glycans

a, Neutralization by 35O22 plateaus below 80% against several pseudoviruses. **b**, Neutralization activity of mAbs against JRCSF pseudoviruses generated in the presence of glycosidase-inhibitors, such as kifunensine (25 μM), NB-DNJ (500 μM) or swainsonine (20 μM). Error bars denote one standard error of the mean (s.e.m.).

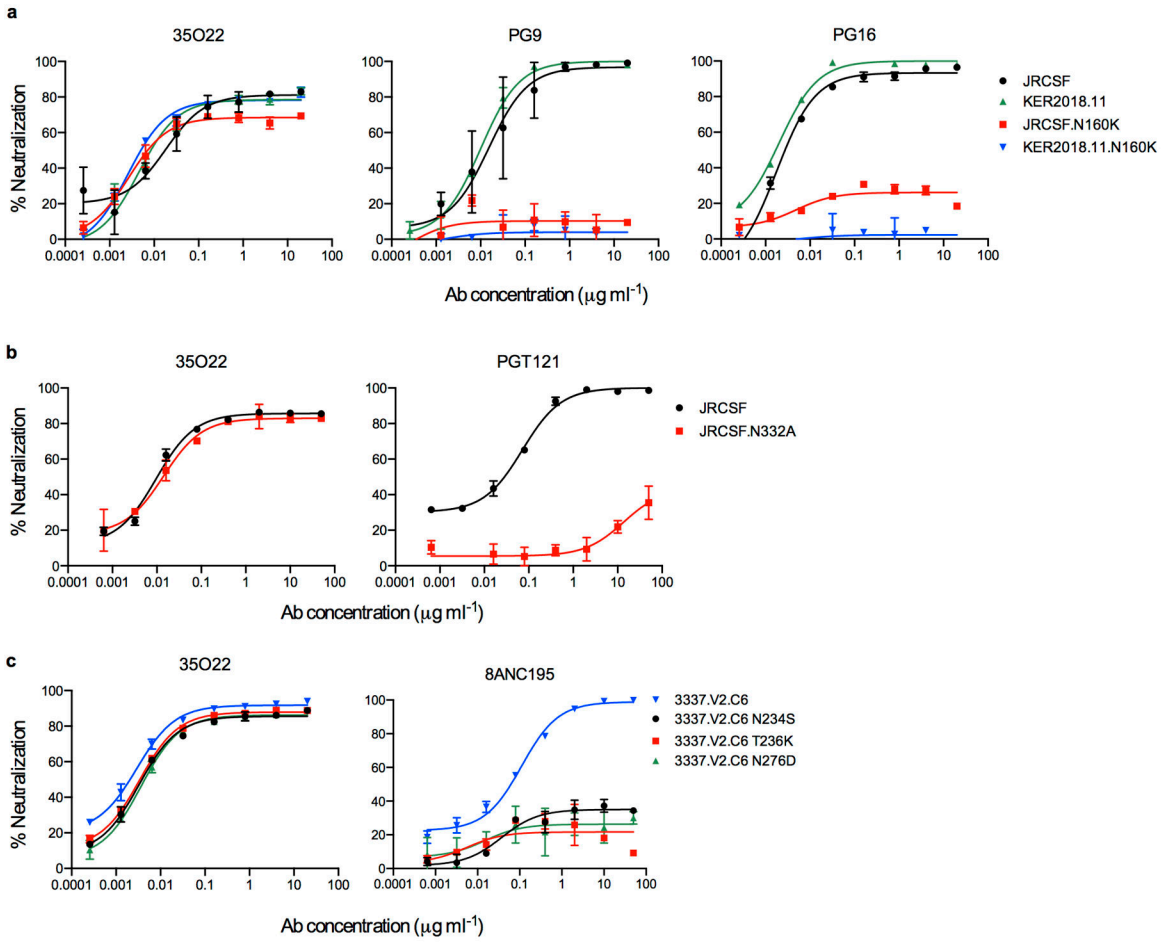

Extended Data Figure 4. Neutralization of 35O22 against pseudovirus mutants known to knock out activity against known glycan-specific antibodies

a, Neutralization of 35O22 against JRCSF or KER2018.11 with or without the N160K mutation. PG9 and PG16 were used as positive controls. **b**, Neutralization of 35O22 against N332A mutants of JRCSF. PGT121 was used as a positive control. **c**, Neutralization of 35O22 against N234S, T236K and N276D mutants of 3337.V2.C6. 8ANC195 was used as a positive control. Error bars denote one standard error of the mean (s.e.m.).

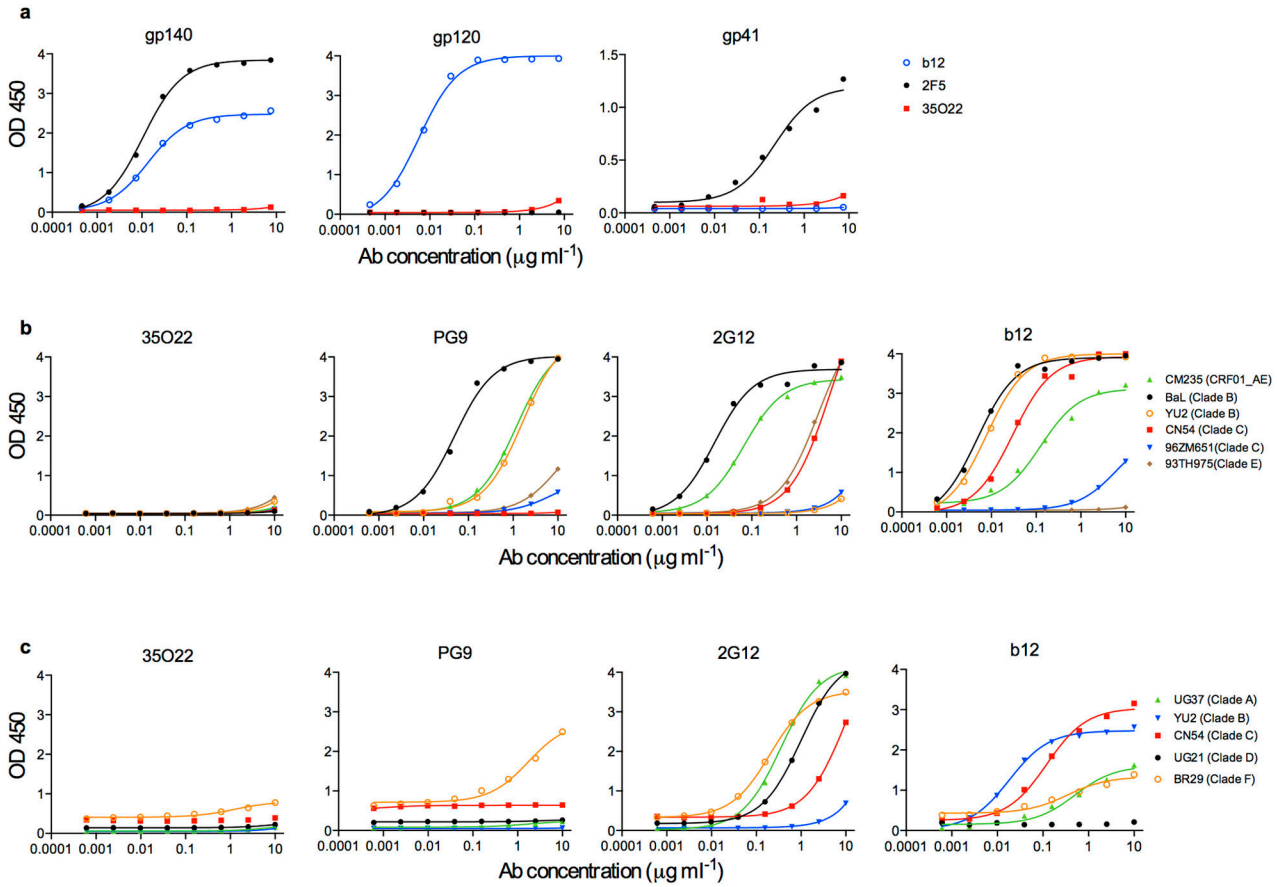

Extended Data Figure 5. Binding specificity of 35O22

ELISA binding of indicated mAbs to HIV_{YU2} gp140 foldon trimer, gp120, and gp41 monomers (**a**). ELISA binding of gp120 (**b**) and gp140 (**c**) monomers from different HIV-1 subtypes.

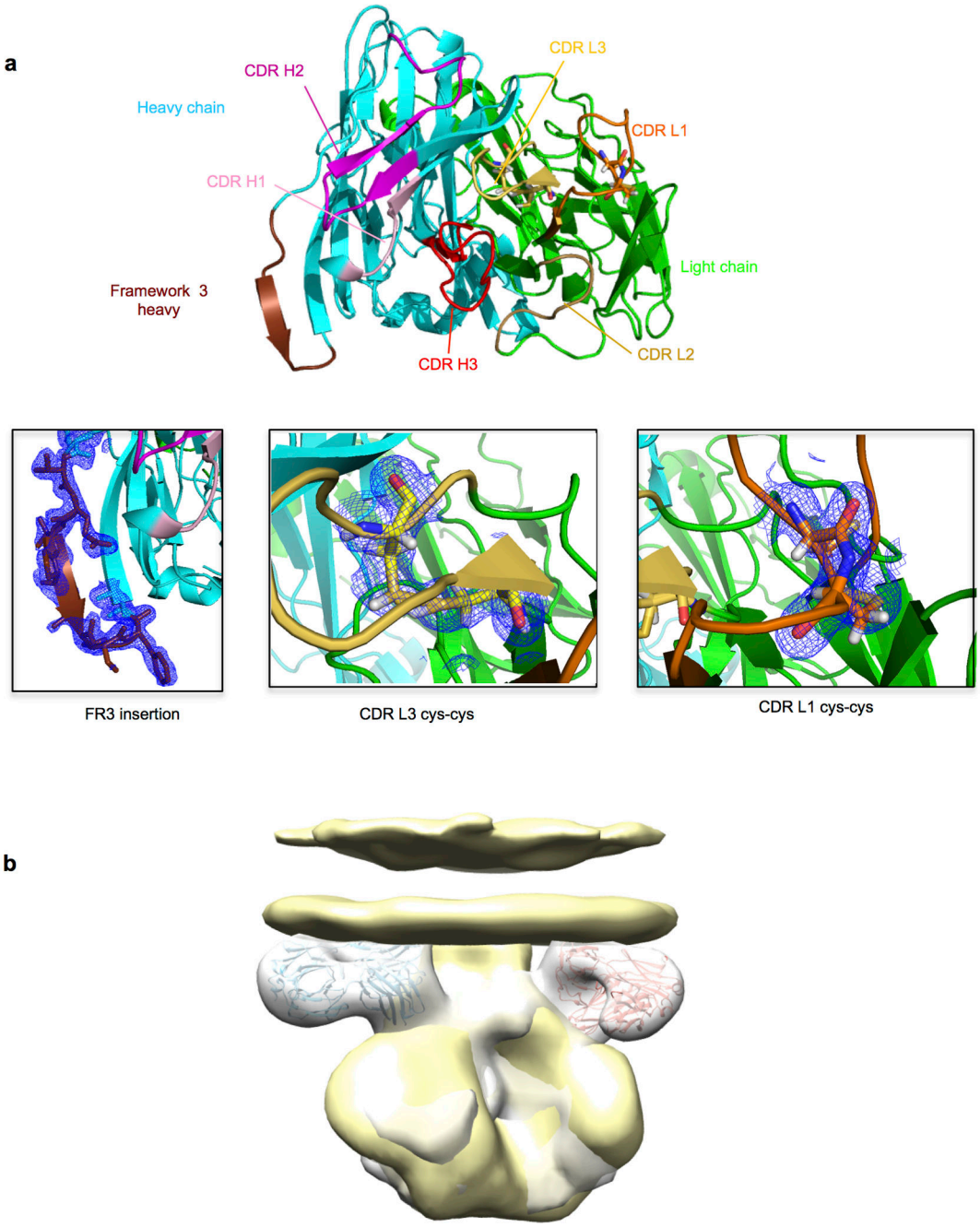

Extended Data Figure 6. 35022 Fab features

a. 35022 is seen looking down on the combining site from the viewpoint of antigen in ribbons with the CDR colored as in Figure 3a. Insets show structural details of the framework 3 insertion, disulfides in CDR L1 and CDR L3 with electron density $2F_0-F_c$ contoured at 1σ.Location of the viral membrane. **b**. Superposition of BaL gp160 negative stain (yellow surface) with the negative stain reconstruction of soluble BG505 SOSIP in complex with 35O22 (grey surface) gives an estimation of the viral membrane location relative to 35O22 antibody as shown in Figure 3b.

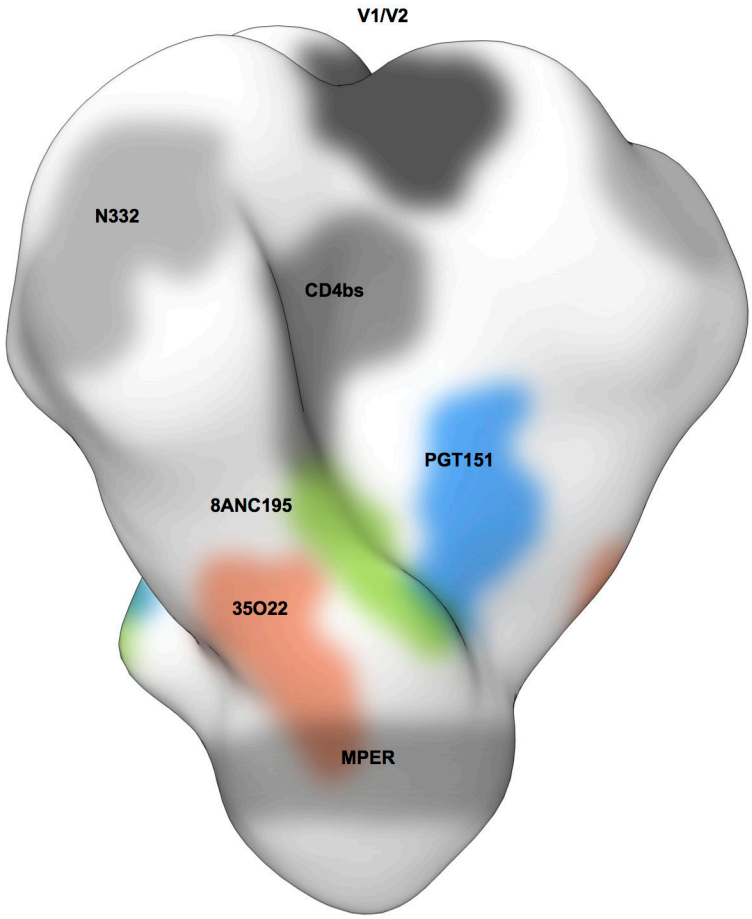

Extended Data Figure 7.
Binding site of 35O22 on the HIV Env trimer. Binding site of 35O22 (red) relative to those of PGT151 (blue) or 8ANC195 (green) are shown.

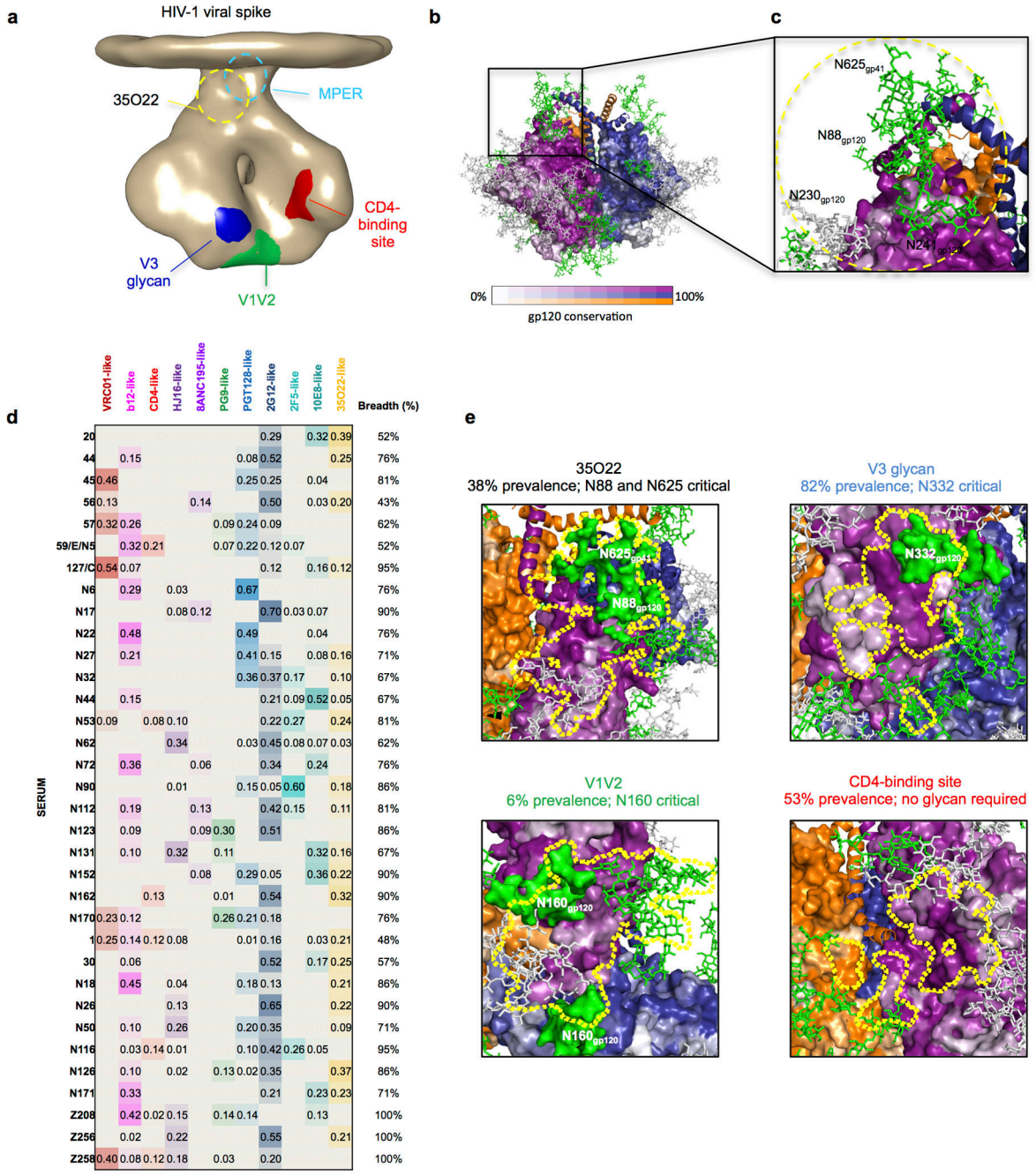

Extended Data Figure 8. A new site of HIV-1 vulnerability at the interface of gp120 and gp41 and prevalence of targeting

a, Dominant sites of vulnerability to neutralizing antibody elicited by natural infection, shown in the context of an EM tomogram from the BAL viral spike. The viral membrane is positioned at the top of the spike. It is unclear if 35O22 and MPER antibodies bind to this form of the viral spike, and approximate locations for these are shown in dotted outlines. **b**, Viral spike from the soluble BG505 SOSIP context, shown in the same orientation as **a**, with gp120 surface colored by conservation from 0–100%, from 4265 HIV-1 strains (white to

purple for protomer 1 with scale shown, white to blue for protomer 2 and white to orange for protomer 3), with glycans shown in green when present in more than 90% of strains, in grey when present in 30–90% of strains and not shown otherwise. **c**, 35O22-identified site of HIV-1 vulnerability, comprises both conserved amino acids and a cluster of glycans, including N88 from gp120 and N625 from gp41. N230 and N241 are not present in BG505 strain. The 35O22 epitope is shown in yellow dotted line. **d**, Neutralization fingerprints for 35O22 and for antibodies encompassing ten different epitope specificities representing the other four known major sites of Env vulnerability were used to interrogate the serum specificities of 34 HIV-infected patients. Values (with proportional color intensities) predict the fraction of serum neutralization that can be attributed to each antibody specificity. Possible 35O22-like signals were predicted for 13 of the sera (values >0.2), while strong signals were observed in 3 of the sera (values >0.3). A panel of 21 HIV-1 strains was used in the neutralization analysis and for computing serum breadth. **e**, Sites of HIV-1 vulnerability to neutralizing antibody outlined by a yellow line. Prevalence in 34-donor cohort indicated along with critical glycans.

Extended Data Figure 9. Autologous virus Env sequence and the impact of variants on 35O22 neutralization

a, A total of 12 single-genome amplicons from plasma of patient N152 were sequenced. Donor Env sequences together with the reference sequences of JRCSF and LAI are aligned. Amino acids critical for 35O22 neutralization of JRCSF and LAI are labeled in yellow. Differences between autologous and JRCSF sequences are labeled in green. **b**, 35O22

neutralization of JRCSF pseudovirus or variants containing the autologous virus mutations from patient N152. Error bars denote one standard error of the mean.

Extended Data Table 1

Neutralizing activity of sera or mAb against HIV_{JRCSF} pseudovirus with mutation in the 35O22 epitope

	ID50					Fold change*			
Sera ID	**WT**	**N88A**	**N230A**	**N241A**	**N625A**	**N88A**	**N230A**	**N241A**	**N625A**
20	6864	7396	5295	5261	5781	0.9	1.3	1.3	1.2
44	6095	2824	1177	2632	776	2.2	5.2	2.3	7.9
45	4019	2422	2094	1678	3265	1.7	1.9	2.4	1.2
56	655	1124	2017	89	1901	0.6	0.3	7.4	0.3
57	7586	626	4981	393	355	12.1	1.5	19.3	21.4
127/C	5217	820	1829	1082	789	6.4	2.9	4.8	6.6
N6	5966	214	437	436	679	27.9	13.7	13.7	8.8
N17	62354	1121	743	2279	1653	55.6	83.9	27.4	37.7
N22	9735	932	3017	1591	3523	10.4	3.2	6.1	2.8
N32	3131	539	1238	2538	686	5.8	2.5	1.2	4.6
N44	5439	1532	2110	2622	2003	3.6	2.6	2.1	2.7
N53	6690	963	1048	352	1044	6.9	6.4	19.0	6.4
N72	6722	1484	1058	199	2482	4.5	6.4	33.8	2.7
N90	4275	3853	1479	1018	10576	1.1	2.9	4.2	0.4
N112	5903	2344	967	706	6071	2.5	6.1	8.4	1.0
N123	21392	1194	1217	771	824	17.9	17.6	27.7	26.0
N131	18777	106	402	163	275	177.1	46.7	115.2	68.3
N152	36636	6677	28758	4339	4279	5.5	1.3	8.4	8.6
N162	17492	558	4078	718	1739	31.3	4.3	24.4	10.1
N170	16472	1342	6564	990	448	12.3	2.5	16.6	36.8
1	3485	1605	343	197	256	2.2	10.2	17.7	13.6
30	14255	5620	3314	13125	6221	2.5	4.3	1.1	2.3
N26	19628	1853	2443	1951	3917	10.6	8.0	10.1	5.0
N18	60183	580	1202	480	656	103.8	50.1	125.4	91.7
N116	586	2504	2176	1948	616	0.2	0.3	0.3	1.0
N27	1088	1446	4656	838	790	0.8	0.2	1.3	1.4
N62	907	536	462	429	263	1.7	2.0	2.1	3.4
N126	2502	1132	1146	3554	1807	2.2	2.2	0.7	1.4
N171	12329	5967	3125	1948	1904	2.1	3.9	6.3	6.5
Z208	21501	9337	4338	8740	1815	2.3	5.0	2.5	11.8
Z256	11467	1584	1881	2055	1240	7.2	6.1	5.6	9.2
Z258	31647	3154	2018	2094	4114	10.0	15.7	15.1	7.7
mAb	**IC50**					**Fold change†**			
10E8	0.078	0.0098	0.01984	0.04513	0.01757	0.13	0.3	0.58	0.23

	ID50					Fold change*			
Sera ID	WT	N88A	N230A	N241A	N625A	N88A	N230A	N241A	N625A
PGT121	0.01508	0.02161	0.02053	0.02399	0.02431	1.43	1.4	1.59	1.61
PG9	0.00692	0.00216	0.0022	0.00189	0.00238	0.31	0.3	0.27	0.34
35O22	0.0106	>20	>20	>20	>20	>1886	>1886	>1886	>1886

*Fold change=ID_{50} of HIV_{JRCSF} WT/ID_{50} of HIV_{JRCSF} mutant. Values with fold changes >5 are highlighted in yellow.

†Fold change=IC_{50} of HIV_{JRCSF} mutant/IC_{50} of HIV_{JRCSF} WT. Values with fold changes >5 are highlighted in yellow.

Supplementary Material

Refer to Web version on PubMed Central for supplementary material.

Acknowledgments

We thank John P. Moore for experiments using the BG505 SOSIP trimer, discussions of experimental data, and careful review of this manuscript. We thank K. Lloyd. R. Parks, J. Eudailey and J. Blinn for performing autoantibody assays. This project has been funded in part with federal funds from the Intramural Research Programs of NIAID, National Institutes of Health. This work was also supported by the NIH HIVRAD grant P01 AI082362, and by the Aids Fonds Netherlands, grants #2011032 and 2012041. R.W.S. is a recipient of a Vidi grant from the Netherlands Organization for Scientific Research (NWO) and a Starting Investigator Grant from the European Research Council (ERC-StG-2011-280829-SHEV). J.M.B. is supported by NIH grants AI93278 and AI84714. Use of sector 22 (Southeast Region Collaborative Access team) at the Advanced Photon Source was supported by the US Department of Energy, Basic Energy Sciences, Office of Science, under contract number W-31-109-Eng-38.

References

1. Kwong PD, Mascola JR. Human antibodies that neutralize HIV-1: identification, structures, and B cell ontogenies. Immunity. 2012; 37:412–425. [PubMed: 22999947]
2. Doria-Rose NA, et al. Breadth of human immunodeficiency virus-specific neutralizing activity in sera: clustering analysis and association with clinical variables. J Virol. 2010; 84:1631–1636. [PubMed: 19923174]
3. Sather DN, et al. Factors associated with the development of cross-reactive neutralizing antibodies during human immunodeficiency virus type 1 infection. J Virol. 2009; 83:757–769. [PubMed: 18987148]
4. Walker LM, et al. A limited number of antibody specificities mediate broad and potent serum neutralization in selected HIV-1 infected individuals. PLoS Pathog. 2010; 6:e1001028. [PubMed: 20700449]
5. Simek MD, et al. Human immunodeficiency virus type 1 elite neutralizers: individuals with broad and potent neutralizing activity identified by using a high-throughput neutralization assay together with an analytical selection algorithm. J Virol. 2009; 83:7337–7348. [PubMed: 19439467]
6. Gray ES, et al. Antibody specificities associated with neutralization breadth in plasma from human immunodeficiency virus type 1 subtype C-infected blood donors. J Virol. 2009; 83:8925–8937. [PubMed: 19553335]
7. Walker LM, et al. Broad and potent neutralizing antibodies from an African donor reveal a new HIV-1 vaccine target. Science. 2009; 326:285–289. [PubMed: 19729618]
8. Wu X, et al. Rational design of envelope identifies broadly neutralizing human monoclonal antibodies to HIV-1. Science. 2010; 329:856–861. [PubMed: 20616233]
9. Huang J, et al. Isolation of human monoclonal antibodies from peripheral blood B cells. Nat Protoc. 2013; 8:1907–1915. [PubMed: 24030440]

10. Tiller T, et al. Efficient generation of monoclonal antibodies from single human B cells by single cell RT-PCR and expression vector cloning. Journal of immunological methods. 2008; 329:112–124. [PubMed: 17996249]
11. Scheid JF, et al. Broad diversity of neutralizing antibodies isolated from memory B cells in HIV-infected individuals. Nature. 2009; 458:636–640. [PubMed: 19287373]
12. Bonsignori M, et al. Two distinct broadly neutralizing antibody specificities of different clonal lineages in a single HIV-1-infected donor: implications for vaccine design. J Virol. 2012; 86:4688–4692. [PubMed: 22301150]
13. Walker LM, et al. Broad neutralization coverage of HIV by multiple highly potent antibodies. Nature. 2011; 477:466–470. [PubMed: 21849977]
14. Burton DR, et al. Efficient neutralization of primary isolates of HIV-1 by a recombinant human monoclonal antibody. Science. 1994; 266:1024–1027. [PubMed: 7973652]
15. Muster T, et al. A conserved neutralizing epitope on gp41 of human immunodeficiency virus type 1. J Virol. 1993; 67:6642–6647. [PubMed: 7692082]
16. Scharf L, et al. Antibody 8ANC195 Reveals a Site of Broad Vulnerability on the HIV-1 Envelope Spike. Cell reports. 2014
17. Falkowska E, et al. Broadly Neutralizing HIV Antibodies Define a Glycan-Dependent Epitope on the Prefusion Conformation of gp41 on Cleaved Envelope Trimers. Immunity. 2014; 40:657–668. [PubMed: 24768347]
18. Blattner C, et al. Structural Delineation of a Quaternary, Cleavage-Dependent Epitope at the gp41-gp120 Interface on Intact HIV-1 Env Trimers. Immunity. 2014; 40:669–680. [PubMed: 24768348]
19. Zhang MY, et al. Identification and characterization of a broadly cross-reactive HIV-1 human monoclonal antibody that binds to both gp120 and gp41. PLoS ONE. 2012; 7:e44241. [PubMed: 22970187]
20. Huang J, et al. Broad and potent neutralization of HIV-1 by a gp41-specific human antibody. Nature. 2012; 491:406–412. [PubMed: 23151583]
21. Scheid JF, et al. Sequence and structural convergence of broad and potent HIV antibodies that mimic CD4 binding. Science. 2011; 333:1633–1637. [PubMed: 21764753]
22. Klein F, et al. Somatic mutations of the immunoglobulin framework are generally required for broad and potent HIV-1 neutralization. Cell. 2013; 153:126–138. [PubMed: 23540694]
23. Haynes BF, et al. Cardiolipin polyspecific autoreactivity in two broadly neutralizing HIV-1 antibodies. Science. 2005; 308:1906–1908. [PubMed: 15860590]
24. Mouquet H, et al. Polyreactivity increases the apparent affinity of anti-HIV antibodies by heteroligation. Nature. 2010; 467:591–595. [PubMed: 20882016]
25. Doores KJ, Burton DR. Variable loop glycan dependency of the broad and potent HIV-1-neutralizing antibodies PG9 and PG16. J Virol. 2010; 84:10510–10521. [PubMed: 20686044]
26. Sanders RW, et al. A next-generation cleaved, soluble HIV-1 Env Trimer, BG505 SOSIP.664 gp140, expresses multiple epitopes for broadly neutralizing but not non-neutralizing antibodies. PLoS Pathog. 2013; 9:e1003618. [PubMed: 24068931]
27. Ringe RP, et al. Cleavage strongly influences whether soluble HIV-1 envelope glycoprotein trimers adopt a native-like conformation. Proceedings of the National Academy of Sciences of the United States of America. 2013; 110:18256–18261. [PubMed: 24145402]
28. Georgiev IS, et al. Delineating antibody recognition in polyclonal sera from patterns of HIV-1 isolate neutralization. Science. 2013; 340:751–756. [PubMed: 23661761]
29. Pancera M, Wyatt R. Selective recognition of oligomeric HIV-1 primary isolate envelope glycoprotelins by potently neutralizing ligands requires efficient precursor cleavage. Virology. 2005; 332:145–156. [PubMed: 15661147]
30. Crooks ET, et al. Characterizing anti-HIV monoclonal antibodies and immune sera by defining the mechanism of neutralization. Human antibodies. 2005; 14:101–113. [PubMed: 16720980]
31. Tong T, Crooks ET, Osawa K, Binley JM. HIV-1 virus-like particles bearing pure env trimers expose neutralizing epitopes but occlude nonneutralizing epitopes. J Virol. 2012; 86:3574–3587. [PubMed: 22301141]

32. Li M, et al. Human immunodeficiency virus type 1 env clones from acute and early subtype B infections for standardized assessments of vaccine-elicited neutralizing antibodies. J Virol. 2005; 79:10108–10125. [PubMed: 16051804]
33. Chakrabarti BK, et al. Direct antibody access to the HIV-1 membrane-proximal external region positively correlates with neutralization sensitivity. J Virol. 2011; 85:8217–8226. [PubMed: 21653673]
34. Binley JM, et al. Redox-triggered infection by disulfide-shackled human immunodeficiency virus type 1 pseudovirions. J Virol. 2003; 77:5678–5684. [PubMed: 12719560]
35. Chuang GY, et al. Residue-level prediction of HIV-1 antibody epitopes based on neutralization of diverse viral strains. J Virol. 2013; 87:10047–10058. [PubMed: 23843642]
36. Pancera M, et al. Soluble mimetics of human immunodeficiency virus type 1 viral spikes produced by replacement of the native trimerization domain with a heterologous trimerization motif: characterization and ligand binding analysis. J Virol. 2005; 79:9954–9969. [PubMed: 16014956]
37. Yasmeen A, et al. Differential binding of neutralizing and non-neutralizing antibodies to native-like soluble HIV-1 Env trimers, uncleaved Env proteins, and monomeric subunits. Retrovirology. 2014 in press.
38. McLellan JS, et al. Structure of HIV-1 gp120 V1/V2 domain with broadly neutralizing antibody PG9. Nature. 2011; 480:336–343. [PubMed: 22113616]
39. Otwinowski Z, Minor W. Processing of X-ray diffraction data collected in oscillation mode. Macromolecular Crystallography, Pt A. 1997; 276:307–326.
40. McCoy AJ, et al. Phaser crystallographic software. J Appl Crystallogr. 2007; 40:658–674. [PubMed: 19461840]
41. Winn MD, et al. Overview of the CCP4 suite and current developments. Acta Crystallogr D Biol Crystallogr. 2011; 67:235–242. [PubMed: 21460441]
42. Emsley P, Cowtan K. Coot: model-building tools for molecular graphics. Acta Crystallogr D Biol Crystallogr. 2004; 60:2126–2132. [PubMed: 15572765]
43. Davis IW, et al. MolProbity: all-atom contacts and structure validation for proteins and nucleic acids. Nucleic Acids Res. 2007; 35:W375–383. [PubMed: 17452350]
44. Kong L, et al. Supersite of immune vulnerability on the glycosylated face of HIV-1 envelope glycoprotein gp120. Nat Struct Mol Biol. 2013; 20:796–803. [PubMed: 23708606]
45. Thornburg NJ, et al. Human antibodies that neutralize respiratory droplet transmissible H5N1 influenza viruses. The Journal of clinical investigation. 2013; 123:4405–4409. [PubMed: 23999429]
46. Julien JP, et al. Crystal structure of a soluble cleaved HIV-1 envelope trimer. Science. 2013; 342:1477–1483. [PubMed: 24179159]
47. Liu J, Bartesaghi A, Borgnia MJ, Sapiro G, Subramaniam S. Molecular architecture of native HIV-1 gp120 trimers. Nature. 2008; 455:109–113. [PubMed: 18668044]

a

35O22 Heavy Chain

IGHV[a]	IGHD	IGHJ	CDR3 length (amino acid)	VH mutation frequency (nt)
1-18*02	5-24*01	4*02 or 4*03	16	96/276 (35%)

35O22 Light Chain

IGLV	IGLJ	CDR3 length (amino acid)	VL mutation frequency (nt)
2-14*02, or 2-23*01, or 2-23*02, or 2-23*03	1*01	10	71/288 (24%)

[a] Germline alleles were determined using the IMGT database (http://imgt.org)

b

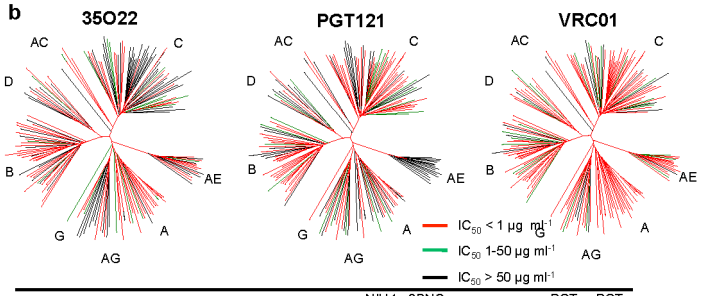

	35O22	10E8	4E10	VRC01	NIH4 5-46	3BNC 117	PG9	PG16	PGT 121	PGT 128
No. of viruses	181	180	180	177	180	180	177	177	177	177
IC_{50} <50 µg ml^{-1}	62%	98%	98%	89%	85%	84%	78%	73%	64%	63%
IC_{50} <1 µg ml^{-1}	49%	72%	37%	75%	76%	77%	65%	59%	51%	50%
Geometric Mean IC_{50}*	0.056	0.22	1.3	0.250	0.138	0.09	0.11	0.06	0.05	0.07
Median IC_{50}	0.033	0.35	1.94	0.248	0.141	0.07	0.09	0.02	0.022	0.027

* Concentration is µg ml^{-1}

Figure 1. Analyses of 35O22 sequence and neutralization

a, Inferred germline genes encoding the variable regions 35O22. **b**, Neutralizing activity of antibodies against a 181-isolate Env-pseudovirus panel. Dendrograms indicate the gp160 protein distance of HIV-1 primary isolate Env glycoproteins. Data below the dendrogram show the number of tested viruses, the percentage of viruses neutralized and the geometric mean or median IC_{50} for viruses neutralized with an IC_{50} < 50 µg ml^{-1}.

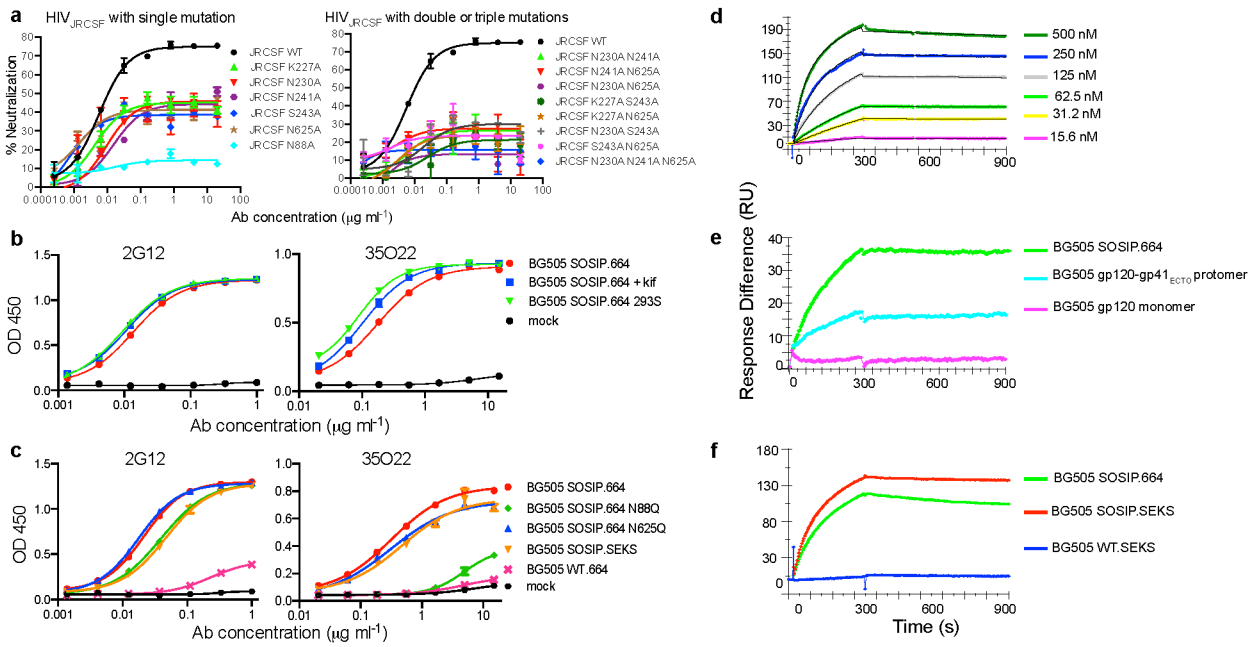

Figure 2. Binding specificity of 35O22

a, Neutralization of HIV_{JRCSF} pseudovirus or variants containing the indicated mutations. **b**, Binding to BG505 SOSIP.664 trimer produced in cells treated with kifunensine or deficient in glycan processing (293S). **c**, Binding to BG505 trimers with the indicated mutations. BG505 SOSIP.SEKS lacks the furin cleavage site. BG505 WT.664 lacks stabilizing mutations and the antigen primarily represents gp41. **d,** SPR analysis of binding to immobilized BG505 SOSIP.664 trimers. **e,** Binding of 35022 (250 nM) to BG505 SOSIP. 664 trimers, gp120-$gp41_{ECTO}$ protomers, or monomeric gp120. **f**, Binding to BG505 SOSIP. 664, BG505 SOSIP.SEKS, or the BG505 WT.SEKS lacking the SOSIP mutations.

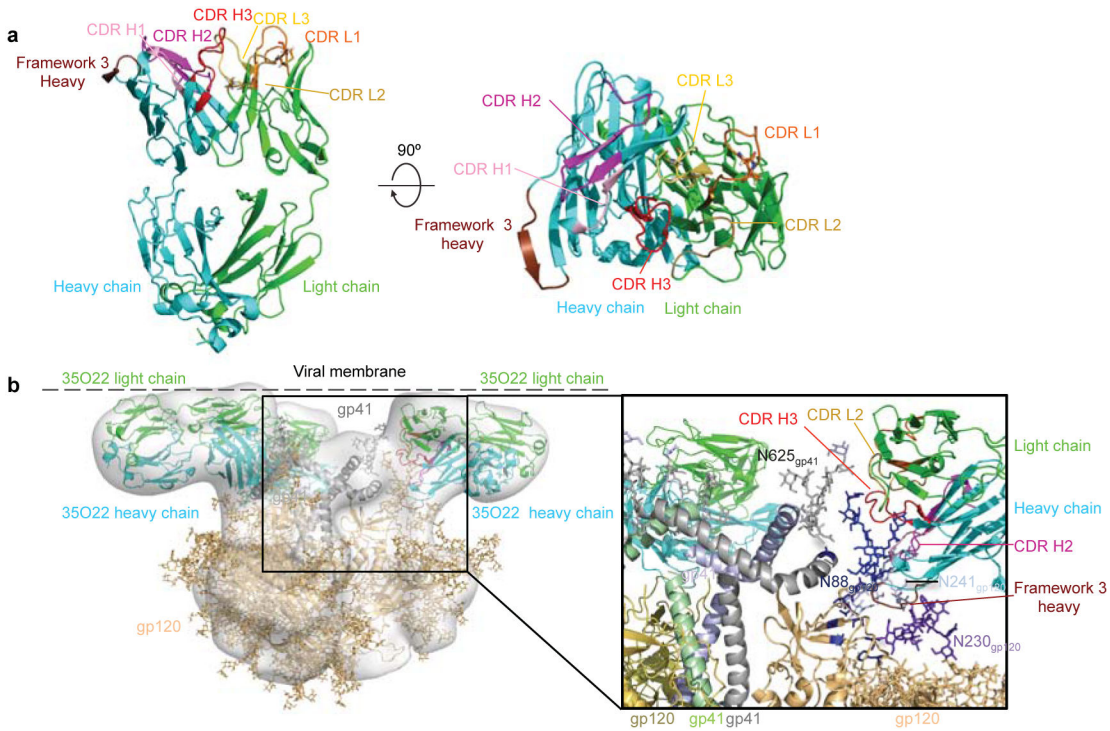

Figure 3. Structure of Fab 35O22 and EM reconstruction of complex with HIV-1 Env

a, Cartoon representation (left) of unbound 35O22 Fab. Heavy chain is in cyan, light chain in green, and the heavy chain FR3 insertion in chocolate. (right) 90° rotation, looking down on combining site. **b**, EM reconstruction of BG505 SOSIP.664 in complex with 35O22 Fab, with fitted crystal structures. gp120 (light orange) and gp41 (grey) shown with 35O22 (as in **a)**. The approximate location of the viral membrane is indicated. Glycans N241 and N230 are not part of the BG505 sequence, but have been modelled for reference.

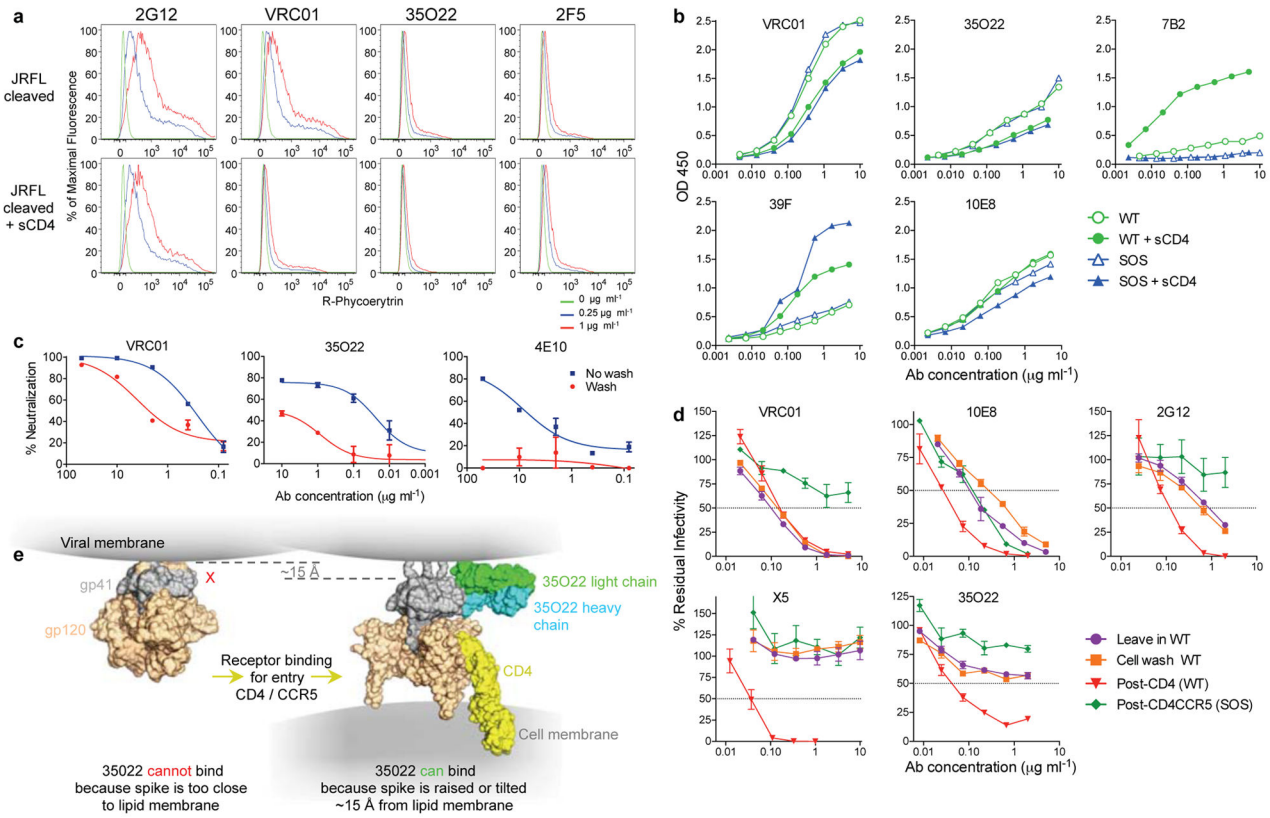

Figure 4. Binding or neutralization in the context of a lipid membrane

a, Staining of cell surface expressed HIV_{JRFL} Env. **b**, ELISA assay of antibody binding to WT or SOS HIV_{JRFL} VLPs. The CD4-inducible 39F antibody or gp41-specific 7B2 are used as controls. **c**, Access to the HIV_{JRFL} Env trimer on pseudovirions based upon washing the antibody-pseudovirion mixture prior to infecting cells. **d,** Kinetic assay of HIV_{JRFL} neutralization. See Methods for a description of individual formats. **e**, Schematic of conformational change resulting in raising of the trimer spike required to permit access of 35O22 to its epitope.